PHYC30170: Advanced Laboratories

Compton Scattering

February 2, 2021

Author: Owen Johnson
Student ID: 18305971
Supervisor: Prof. Luis León Vintró

UCD School of Physics
Scoil na Fisice UCD

Disclaimer

Due to the circumstances surrounding COVID-19 restrictions the data used throughout the duration of this report was provided by the UCD Department of Physics such that the lab could be completed remotely.

Abstract

The investigation aimed to explore Compton scattering phenomenon and relate it in a relativistic context. This was done in two separate investigations. The first investigation demonstrated that gamma rays' energy had a linear relationship to the angle in which they were scattered. It was also shown that the experimental data was in-line with theoretical predictions. This was then further expanded on by comparing the differential cross-section of the experimental data to the Klein–Nishina prediction this also yielded a result in line with theoretical models with an average difference of 1.4% on each data point. The second investigation explored Compton scattering in a relativistic sense. This was done with a multitude of radioactive sources to compare the electron's rest energy. It was found that when this was determined in a non-relativistic context, a linear relationship was observed with the y-intercept of 0.514 ± 0.004 MeV—calculating the rest energy in a relativistic context produced a result of 0.515 ± 0.007 MeV. It was further demonstrated by the dependence that energy and momentum had on the velocity of the electron.

Contents

1 Introduction **1**

2 Theory **1**

2.1 Evaluation of Scattered Gamma Ray Energies and Cross Section 1

2.2 Compton Scattering & its Relativistic Relations 3

2.2.1 Classical Approach to Determination of Electron Rest Mass 3

2.2.2 Relativistic Approach to Determination of Electron Rest Mass 4

2.2.3 Relativistic Relations as a Result of Relativistic Rest Mass 4

3 Experimental Apparatus **5**

4 Experimental Methodology **6**

4.1 Evaluation of Scattered Gamma Ray Energies and Cross Section 6

4.2 Compton Scattering & its Relativistic Relations 7

5 Results **8**

5.1 Scattered Gamma Ray Energies and Cross Section 8

5.2 Compton Scattering & its Relativistic Relations 10

5.3 Relativistic Relations 12

6 Conclusion **15**

A Constants used throughout investigation **17**

B Raw Data **19**

C Derivation of Compton Scattering Equation **20**

D Relevant Code Used **21**

D.1 Code used for evaluation of scattered gamma ray energies and cross section. 21

D.2 Code used for investigating relativistic relations 25

1 Introduction

The Compton effect was brought to fruition by Arthur H. Compton in a research paper published in 1923. Before this paper was published, it was observed that X-Ray's of a known wavelength interacted with atoms they would emerge from the interaction with a different angle of the path before the interaction. It also had varied shorter wavelengths, thus losing energy, conservation of energy dictated that the energy must be accounted for. In classical physics, it was postulated that the wavelengths should remain the same after this interaction. In Compton's study, he proposed reasoning for this phenomenon by relating light to particle motion and applying conservation laws to the problem. This study was further evidence of why light needed to be considered both a wave and a particle. [1]

Compton scattering is a key importance in the field of radiobiology as the interactions of gamma rays and high energy x-rays are an essential part of things such as radiation therapy. It also plays a role in gamma spectroscopy as it explains the Compton edge and gives appropriate ways to counteract this effect. It is also used heavily in material physics to probe electrons' wave function present in matter when representing momentum. [2–4]

The aim of this experiment is to demonstrate the results of Compton scattering for gamma rays that get scattered at various angles. The experiment always explores the short-comings of a non-relativistic model for Compton scattering and how when relativistic effects are taken into account a more accurate picture of Compton scattering is obtained.

2 Theory

This investigation is split up into multiple sections with various subsections. The first use of conventional means to show the effect Compton interactions have as a function of incident angle. With the second section exploring the results when taking into account relativistic effects and factors resulting from Compton interactions.

2.1 Evaluation of Scattered Gamma Ray Energies and Cross Section

The first part of this investigation studies gamma rays' energy along with their differential cross-section as they are measured against their scattering angle.
To perform this study, it is first required to obtain mathematical expressions that detail Compton scattering. To do this, we first start with the situation we see in fig. 2.1.

In fig. 2.1 a gamma-ray of energy E_γ scatters from an electron with an energy of $E_{\gamma'}$, with the angle between them (angle of scattering) denoted by θ. During this interaction, conservation laws must be obeyed, so energy is conserved in the system. The following equation describes the conservation of energy,

$$E_\gamma = E_{\gamma'} + E_e \tag{2.1}$$

The momentum in both the x and y directions can be described by the following two equation[1],

[1] Where m_0 is the rest mass of the electron, v is the velocity of recoiled electron and other variables have their usual meaning.

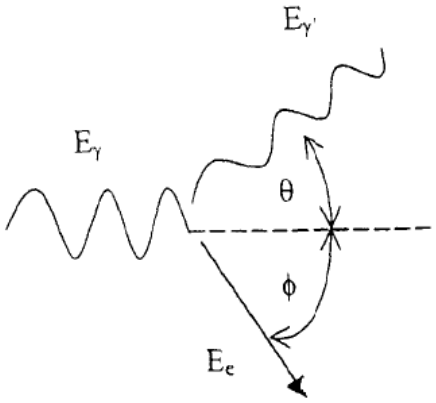

Figure 2.1 *The scattering that is caused by Compton interaction [5]*

$$\frac{hf}{c} = \frac{hf'}{c}\cos\theta + mv\cos\phi \qquad \text{(x-direction)} \tag{2.2}$$

$$0 = \frac{hf'}{c}\sin\theta - mv\sin\phi \qquad \text{(y-direction)} \tag{2.3}$$

Where in the above equation Planck-Einstein relation is used to relate energy to frequency ($E = hf$), the electron energy E_0 is give by $E_e = mc^2 - m_0c^2$ and m is given by, $m = m_0/(1 - v^2/c^2)^{-1/2}$. Using these expressions in conjunction a expression for electron energy ($E_{\gamma'}$) as follows,

$$E_{\gamma'} = \frac{E_\gamma}{1 + \frac{E_\gamma}{m_0c^2}(1 - \cos\theta)} \tag{2.4}$$

From eq. (2.4) it's possible to create a theoretical model to compare obtained experimental data during analysis. This is done using the values for E_γ and m_0c^2 when using the Caesium-137 $\left(^{137}\text{Cs}\right)$ source in the lab. The values for E_γ and m_0c^2 are 0.662 MeV and 0.551 MeV respectively. Using these values in eq. (2.4) the following is obtained,

$$E_{\gamma'} = \frac{0.662}{1 + 1.295(1 - \cos\theta)} \tag{2.5}$$

Now with the use of eq. (2.5), it is possible to obtain theoretical predictions as long as the angle θ is known. This will be very useful for analysis on experimental data which will be seen in section 5.1. With the expressions above, it is now possible to demonstrate the effects of Compton scattering as a function of angle θ using experimental data.

It is also possible to determine the probability that an incident photon is Compton scattered at an angle θ, this is known as the differential cross-section for Compton scattering. Determining the differential cross-section is an appropriate way to demonstrate Compton scattering. The Klein–Nishina formula gives the differential cross-section of photons scattered from a single free electron and can be used as a theoretical model to compare experimental data to. The differential cross-section according to the Klein–Nishina equation is given by the

following expression, [5, 6]

$$\left(\frac{d\sigma}{d\Omega}\right)_{\text{theory}} = \frac{r_0^2}{2}\left\{\frac{1+\cos^2\theta}{[1+\alpha(1-\cos\theta)]^2}\right\}\left\{1+\frac{\alpha^2(1-\cos\theta)^2}{(1+\cos^2\theta)(1+\alpha[1-\cos\theta])}\right\} \tag{2.6}$$

r_0 is the classical electron radius, $d\Omega$ is the measured angle in radians, and $\alpha = E_\gamma/m_0c^2$ for further details the constants and numerical values used throughout this section, please see appendix A.
The following expression can be then used to determine the differential cross-section using experimental data.

$$\left(\frac{d\sigma}{d\Omega}\right)_{\text{experimental}} = \frac{\sum_\gamma'}{N\Delta\Omega I} \tag{2.7}$$

Full discussion of variable and constants values for **??** can be found in appendix A.

2.2 Compton Scattering & its Relativistic Relations

Using high energy gamma rays subject to Compton scattering in the lab gives a good opportunity to explore the relativistic relations between the process and the recoiling electron as described in section 2.1.

The data obtained to carry out this section of the investigation is done by measuring the kinetic energy of the recoiling electron when the incident gamma-ray is scattered at 2π radians, this is known as the Compton Edge and denoted by T.

2.2.1 Classical Approach to Determination of Electron Rest Mass

It is a good place to start when analysing relativistic relations if a phenomenon is looking at what the classical theory dictates. With a couple of simple ideas, it is possible to obtain expressions that will allow the Compton edge and gamma-ray relation to an electron's rest mass.
Here, like anywhere in physics, the laws of conservation hold firm, the classical relationship for energy and an electromagnetic wave is used ($E_\gamma = p_\gamma c$). The Compton edge is equivalent to an electron's kinetic energy, which is subjected to an incident gamma-ray at 2π radians.
Applying the law of conservation of momentum to this setup the following is obtained,

$$p_\gamma = p - p_\gamma^{'} \tag{2.8}$$

where p_γ, p and $p_\gamma^{'}$ are the momentum of incident gamma ray, scattered gamma ray and recoiling electron. Doing the same for conservation of energy yields,

$$p_\gamma c = p_\gamma^{'} + T \tag{2.9}$$

Combing the results from and the following is obtained,

$$pc = 2E_\gamma - T \tag{2.10}$$

Assuming the following non-relativistic relationship, we can put eq. (2.10) into terms that use experimental data that can be obtained in the lab[2].

[2]Note, the nr subscript stands for non-relativistic wherever it appears.

$$T = \frac{p^2}{2m_{nr}}$$

Using the above expression and solving for rest energy the following is obtained[3],

$$m_{nr}c^2 = \frac{p^2c^2}{2T} = \frac{(2E_\gamma - T)^2}{2T} \tag{2.11}$$

With this, an expression for non-relativistic corrected rest mass can be used in conjunction with experimental data to obtain numeric values that can be compared with relativistic corrected rest masses in order to determine the validity of correction.

2.2.2 Relativistic Approach to Determination of Electron Rest Mass

From further experiments conducted it was found that eq. (2.11) was not sufficient enough to provide a correct value for the electron rest mass as when the results were plotted a linear relationship would form. It was found that replacing eq. (2.11) with an expression derived from the central-energy momentum relationship described by special relativity would yield more promising results as follows,

$$p^2c^2 + (m_0c^2)^2 = (T + m_0c^2)^2 = E^2 \tag{2.12}$$

Where E is the total energy of the electron. Once eq. (2.12) had been derived from the theory of relativity it was possible to solve for rest mass as follows,

$$m_0c^2 = \frac{p^2c^2 - T}{2T} = \frac{2E_\gamma(E_\gamma - T)}{T} \tag{2.13}$$

Now that eq. (2.13) has been obtained it is possible to calculate electron rest mass using experimentally obtained data.

2.2.3 Relativistic Relations as a Result of Relativistic Rest Mass

Now that the electron mass can be determined accounting for relativistic factors it is also possible to determine other relativistic attributes related to the Compton interactions and use these results as another form of rigour to demonstrate why relativistic relationships are needed to explain the full picture.

It's possible to determine electron velocity, (β) by relating the velocity to momentum and energy to obtain the following expression,

$$\beta = \frac{v}{c} = \frac{mvc}{mc^2} = \frac{pc}{E} = \frac{2E_\gamma - T}{T + m_0c^2} = \frac{T(2E_\gamma - T)}{T^2 - 2E_\gamma T + 2E_\gamma^2} \tag{2.14}$$

The total energy of the electron can also be expressed in terms so that it can be calculated using experimental data,

$$E = T + m_0c^2 = \frac{T^2 - 2TE_\gamma + 2E_\gamma}{T} \tag{2.15}$$

[3]Using the mass-energy equivalence relationship for defining rest mass, $E = mc^2$

Finally using the relativistic mass-energy equivalence formula ($E = \gamma m_0 c^2$) a value for the relativistic factor (Lorentz factor) can be calculated using obtained experimental data as follows,

$$\gamma = \frac{E}{m_0 c^2} = \frac{m_0 c^2 + T}{m_0 c^2} = 1 + \frac{T^2}{2E_\gamma (E_\gamma - T)} \tag{2.16}$$

The means for obtaining meaningful results from data that can be obtained in the lab has been established. Now a means to obtained the data must be established. [5, 7]

3 Experimental Apparatus

As described in section 2, the experiment is split up into two separate investigations. For each investigation, there is a change in the apparatus used to carry out the investigation.

For the first section of the investigation, a Thallium activated Sodium Iodide (denoted by NaI(Tl)) detector is used to measure the scattering electrons' energy. The detector contains two notable parts a NaI crystal and a photomultiplier tube (PMT). Once the crystal is activated by the presence of Thallium, it begins to produced scintillations by incident gamma rays which are then amplified by the PMT via a coupled photo-cathode. The scintillations are caused by the ionisation of sodium iodide, this allows for excited states within the crystal to decdecay-causinge 'flash'.[4]

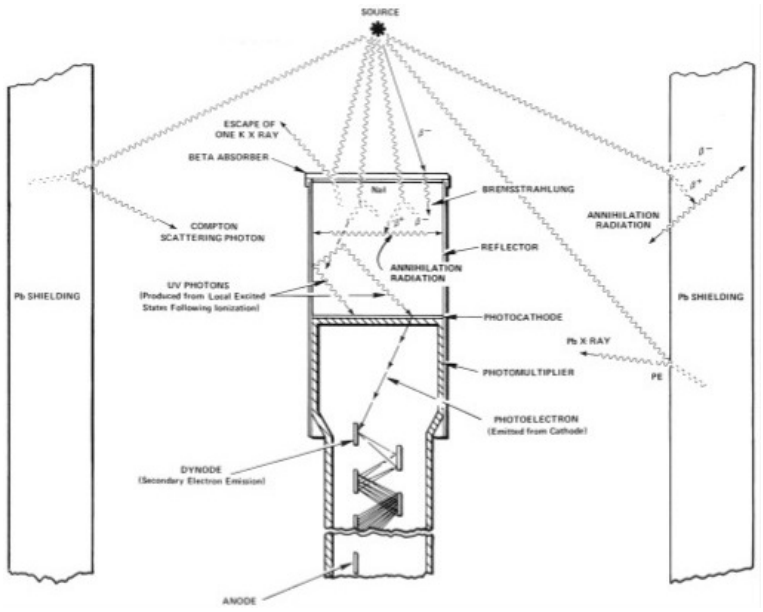

Figure 3.1 *The structure of the NaI(Tl) detector and various types of gamma-ray interactions that occur in the typical source-detector-shield configuration [8]*

The photomultiplier used a high potential and the photoelectric effect to convert the scintillations to pulses. The pulses were then converted into an analogue signal; the signal was then outputted to a computer running

[4] For more information on the technical details of how this works, please see Ref. [8]

a Maestro MCB25 software environment such that the gamma-ray spectrum was recorded. The programme allowed for counts, net-area and counting times to be determined.

For the second part of the experiment, the same software is used the NaI(Tl) detector, however, is swapped out for a Germanium, lithium doped detector (denoted by (Ge(Li))). The swap is that of accuracy the Ge(Li) detector will provide higher resolution. The higher resolution is provided from the presence of a doped semiconductor in the detector. The trade-off of using a semiconductor in the detector is noise, due to the presence of a doped semiconductor, there are impurities in the Ge, causing a lower energy threshold for electron-hold pairs is created. This is negated by having a depletion zone such that more considerable energies are needed to bridge and allow for current to flow[5].

4 Experimental Methodology

As previously outlined, the experiment contains investigations; thus, two experimental procedures were required to obtain all relevant to carry out analysis as outlined in section 2. When working with dangerous sources, all appropriate protection and protocols were followed to protect person(s) conducting the experiment. Each source is placed in a lead box with an adjustable aperture see fig. 4.1.

4.1 Evaluation of Scattered Gamma Ray Energies and Cross Section

The ^{137}Cs source's aperture is placed in line with the scattering sample. The scattering sample is placed on the fulcrum of an arm with the NaI(Tl) detector mounted. The detector can pivot about the scattering sample where the angle, θ can be recorded; see fig. 4.1.

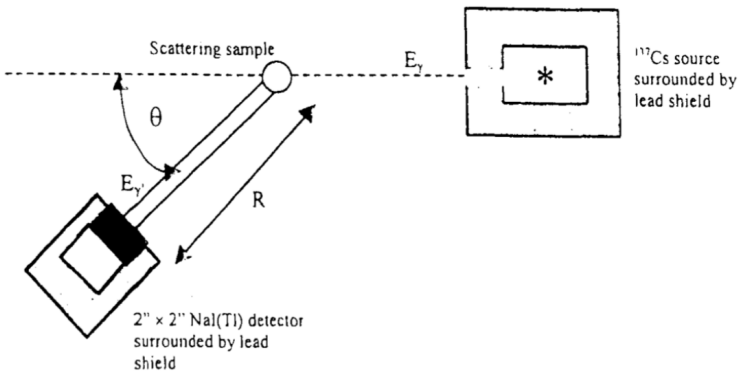

Figure 4.1 *Top down overview of apparatus set up during this investigation [5]*

Before the collection of data begins, the apparatus was calibrated before the lab session. This was done by using the detector to obtain two known gamma spectrums from a different ^{137}Cs sample, and a ^{241}Am sample. The Maestro MCB25 software was then used to calibrate the detector with the gamma-ray spectrum obtained from the sample. After this calibration was completed, data collection commenced.

[5]For a more detailed account of how the Ge(Li) detector operates, please see sections III and IV of Ref. [7]

Setting the arm at an initial angle of 20°and allowing for at least 10,000 counts to register by the Maestro MCB25 software. Then the values for photopeak, counting time and the sum of counts are recorded. This process is then repeated for various values of the angle increasing in increments of 5°until a value of 90°is reached. See table B.1 in appendix B for data recorded from this procedure.

4.2 Compton Scattering & its Relativistic Relations

For carrying out the procedure in the second investigation, numerous sources are used to take readings. However, once again, as in the previous section calibration is required. This is done by taking the background readings for 24 hours before the lab session. The background readings is then subtracted from readings obtained during the lab session using Maestro MCB25. Once this is done, data collection on each of the sources can commence.

Each source was placed and measured until the formation of a clear spectrum; this meant that the Compton edge and photopeak were distinct and easy to identify (see fig. 4.2). In the case of each source the Compton edge and photopeak were recorded, data obtained from this can be found in table B.2 in appendix B.

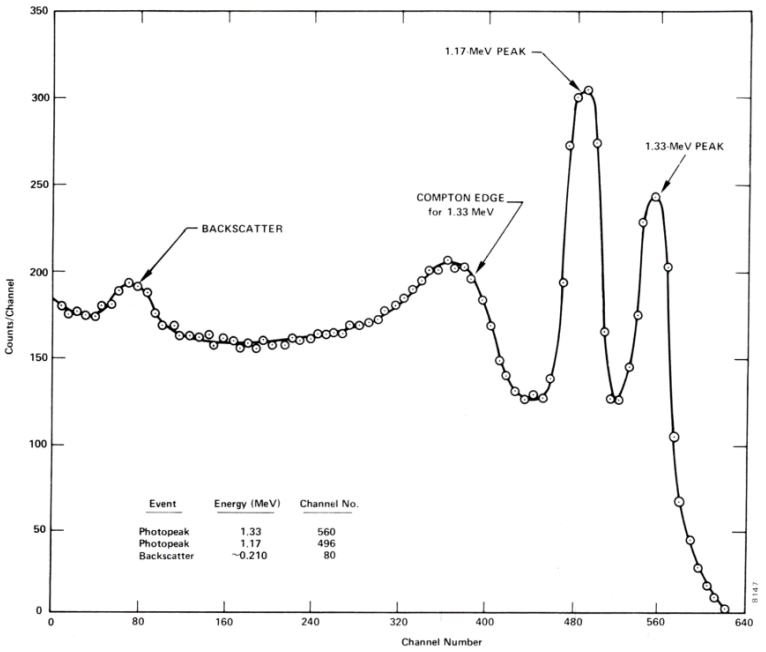

Figure 4.2 *Compton edge of* ^{60}Co *on gamma spectrometer Na(Tl)*

5 Results

5.1 Scattered Gamma Ray Energies and Cross Section

The experiment was carried out as described in section 4.1. The raw results produced in the lab can be found in table B.1. With the use of eq. (2.5) it was possible to re-arrange the expression in the form of a linear fit ($y = mx + c$) as seen below,

$$\frac{1}{E'_\gamma} = 1.51 + 1.956(1 - \cos\theta) \tag{5.1}$$

Below in fig. 5.1, the results that were produced in the lab were plotted along with the theoretical prediction provided by eq. (5.1). As shown in fig. 5.1, the experimental data produced a linear fit in line with that of the theoretical prediction. The experimental data was then linearly fitted such that a value for the slope could be obtained. The slope of the fitted data was found to be $(1.946 \pm 0.007) \times 10^{-26}$ and the y-intercept was found to be $(1.573 \pm 0.063) \times 10^{-26}$.
The value obtained for the slope was 0.005% greater than that of the predicted scope of 1.956×10^{-26} and with the inclusion of experimental uncertainty fell within the expected range. The same was found when observing the y-intercept with the experimental value producing a result that was 0.04% greater than that of the predicted y-intercept if 1.510×10^{-26}, with the inclusion of experimental uncertainty.

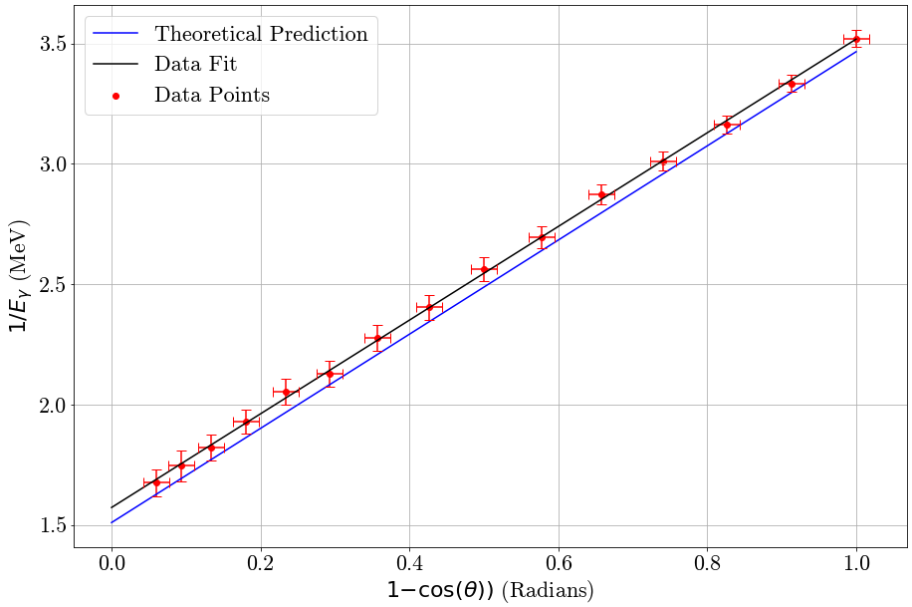

Figure 5.1 *Results of plotting lab data as a function of* $1/E_\gamma$ *against* $1 - \cos\theta$ *for both theoretical and experimental values.*

From this, it is possible to conclude that the gamma-ray's scattering angle and energy display a linear relation that agrees with the theoretical predictions with the inclusion of experimental uncertainties as discussed in section 2.1.
The uncertainties found on the data-points in fig. 5.1 were calculated by propagating the errors on the measurements (see table B.1) through eq. (2.4) to obtain uncertainties on both the x and y values. See

appendix D for more information on how this was completed.
The uncertainty values for both the y-intercept and the slope were taken to be the square-root of their respective covariance matrix diagonals, this calculation is also highlighted in listing?? om appendix D.

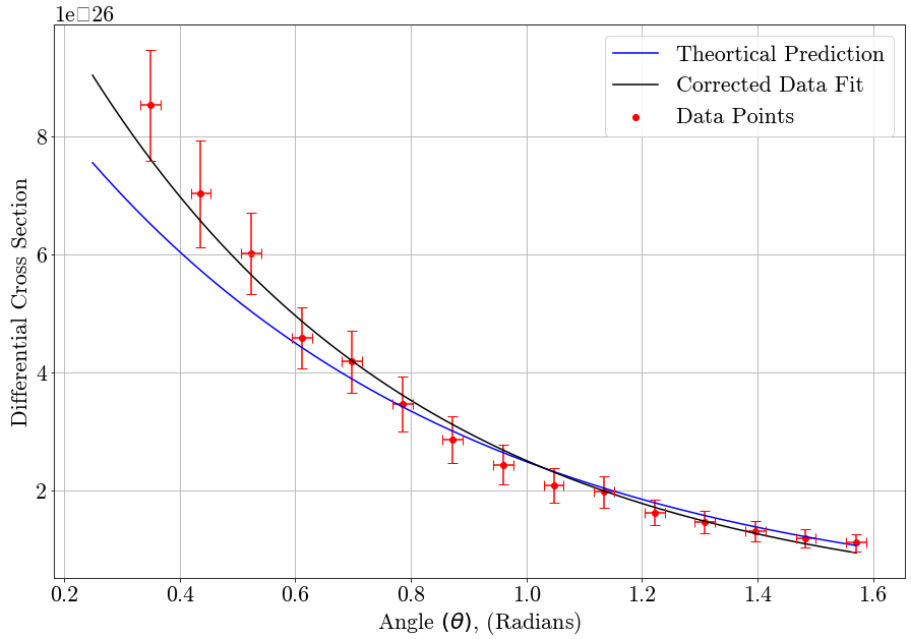

Figure 5.2 *Results of plotting lab data as a function of differential cross section against θ for both theoretical and experimental values.*

Once again using the data from table B.1 the differential cross-section was calculated using eq. (2.7). The results from this can be seen plotted in fig. 5.2 and table 5.1. As evident from both fig. 5.2 and table 5.1, the experimental results and theoretical results are of the same order of magnitude. However, the difference in both experimental results and theoretical results vary significantly at the two ends of the data set, with the smaller angle having the largest difference between theoretical and differential cross-section (see table 5.1). When the data obtained was first plotted the values were corrected by a factor of 11.9 ± 0.4, a possible reason for this could be due to an overestimation in the number of electrons considered or an overestimation of the intensity of the beam, this could occur if the source were partially covered or some other element obstructing the full area to be considered as described by the Klein–Nishina formula.
considering this it would explain the larger variance at either end of the values for angle as we see in fig. 5.2 and table 5.1. This indicates that the experimental data obtained are in line with the theoretical values and large deviance is due to an unforeseen factor in recording the data such as a partially shielded source.

Angle (θ)	Differential Cross Section	Klein–Nishina Cross Section (Theoretical)	Difference (%)
0.349 ± 0.017	8.527 ± 0.936	6.465	31.9
0.436 ± 0.017	7.030± 0.906	5.806	21.1
0.524 ± 0.017	6.017± 0.692	5.132	17.2
0.611 ± 0.017	4.591± 0.517	4.484	2.4
0.698 ± 0.017	4.189± 0.527	3.887	7.8
0.785 ± 0.017	3.467± 0.459	3.359	3.2
0.873 ± 0.017	2.863± 0.395	2.904	-1.4
0.960 ± 0.017	2.437± 0.336	2.522	-3.4
1.047 ± 0.017	2.090± 0.293	2.208	-5.3
1.134 ± 0.017	1.980± 0.264	1.955	1.3
1.222 ± 0.017	1.630± 0.217	1.753	-7.0
1.309 ± 0.017	1.471± 0.187	1.594	-7.8
1.396 ± 0.017	1.319± 0.172	1.472	-10.4
1.484 ± 0.017	1.195± 0.156	1.379	-13.3
1.571 ± 0.017	1.122± 0.150	1.309	-14.3

Table 5.1 *Comparison of experimental and theoretical values for Differential Cross Sections.*

The numerical uncertainties found in both fig. 5.2 and table 5.1 were calculated by propagating the measurement uncertainties found in table B.1 through eq. (2.7).
The 'correction' factor used to adjust the overestimation of the experimental was found by use of the following expression,

$$\text{C.F} = \left\{ \sum_{0}^{n} \frac{\text{Theortical Cross Section}}{\text{Experimental Cross Section}} \right\} \div n \tag{5.2}$$

The error on this value was also found by propagation. The code and methods to complete this can be found in listing?? in appendix D.

5.2 Compton Scattering & its Relativistic Relations

As discussed in section 2.2, the second part of the investigation explores various attributes the energy-momentum relation has when described in the context of special relativity. The first investigation into the relativistic relations looks at the rest energy of recoiling electrons for numerous sources from a non-relativistic and relativistic standpoint. With the use of eq. (2.11) and eq. (2.13), the rest energy was plotted as a function of the sources Compton edge as seen in.

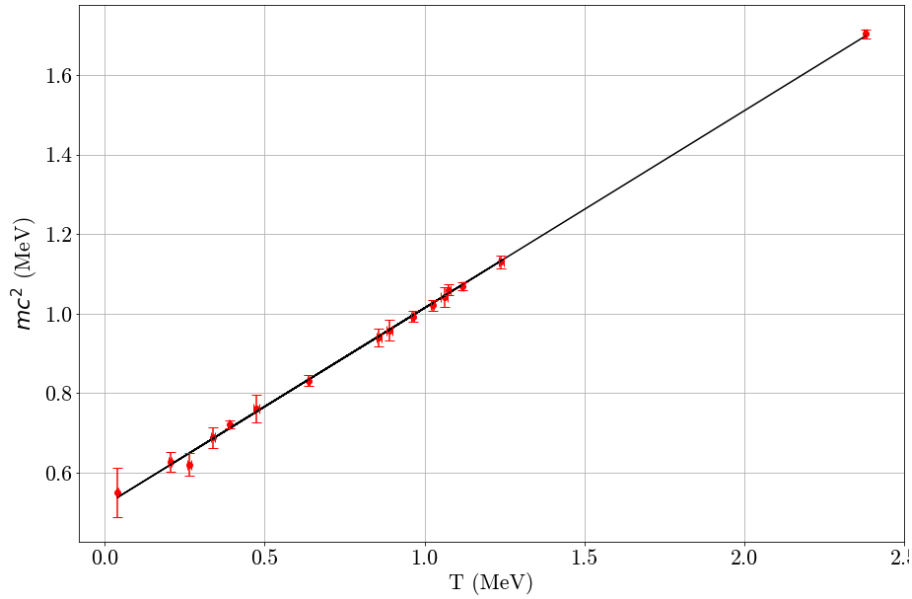

Figure 5.3 *Rest energy plotted as a function of Compton edge*

As evident in fig. 5.3, we can see that the rest mass is showing a linear relationship as the Compton edge increases. This is clearly incorrect as the expected experimental value should remain consistent around the experimentally accepted value for the electrons rest energy of 0.511 MeV. However, when obtaining the slope and y-intercept of the linear fit in fig. 5.3 a value of 0.496 ± 0.005 and 0.518 ± 0.004 respectively. As suggested from the relativistic correction, the classical method's slope should be around 0.5, which is seen here. The y-intercept around the accepted experimental value for rest energy for the electron is also seen here.

Repeating the process using eq. (2.13) to obtain electron rest energy with relativistic correction fig. 5.4. The results observed in this plot are much more in-line with what to expect when measuring electrons' rest energy from varying sources. The average value for the rest energy observed in fig. 5.4 was found to be 0.515 ± 0.007. This value is 0.008 % greater than the expected experimental value and falls within the range of the experimental value when uncertainty is taken into account.

These results work in conjunction with the equation derived for non-relativistic rest energy (eq. (2.11)). When comparing both equations if eq. (2.11) left-hand side is replaced with $m_0c^2 + T/2$ it leads back to the result obtained in eq. (2.12). This result is also further evidence that using relativistic relations provides a more accurate depiction of each source's rest energy.

The errors plotted here were calculated by propagating the error taken on measurement through relevant equations to each result, this process was completed with the use of an uncertainties package with all relevant code found in appendix D.2. However, the values for uncertainties are higher than expected. The expected uncertainty on a particular measurement in fig. 5.4 should be in the range of $0.001 - 0.002$ MeV whereas, for example, Cobalt-57 has an associated uncertainty of 0.06 MeV. The reasons for this disparity is due to an overestimation of the measurement uncertainty on both photopeak and Compton edge. However, the uncertainties still give a high enough degree of precision to determine rest energy. To account for this, when the average rest energy has calculated the uncertainty associated with each value was also propagated, which

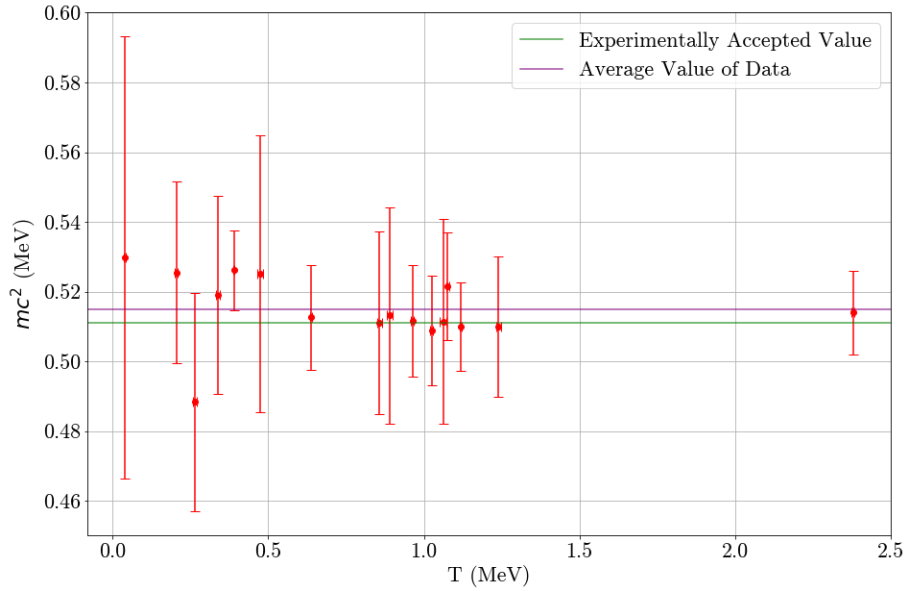

Figure 5.4 *Rest energy plotted as a function of Compton edge*

returned acceptable results.

Source	Compton Edge $(T)(MeV)$	$(m_{nr}c^2)$(MeV)	(mc^2)(MeV)
Na-22	0.338 ± 0.006	0.688 ± 0.026	0.519 ± 0.028
Na-22	1.062 ± 0.010	1.042 ± 0.024	0.511 ± 0.029
K-40	1.240 ± 0.007	1.130 ± 0.017	0.510 ± 0.020
Mn-54	0.637 ± 0.004	0.831 ± 0.013	0.513 ± 0.015
Co-56	1.025 ± 0.005	1.021 ± 0.013	0.509 ± 0.016
Co-57	0.039 ± 0.003	0.549 ± 0.062	0.530 ± 0.063
Co-60	0.963 ± 0.005	0.993 ± 0.014	0.512 ± 0.016
Co-60	1.118 ± 0.004	1.069 ± 0.011	0.510 ± 0.013
In-116	0.263 ± 0.006	0.620 ± 0.029	0.488 ± 0.031
In-116	0.890 ± 0.010	0.958 ± 0.026	0.513 ± 0.031
In-116	1.076 ± 0.005	1.060 ± 0.013	0.522 ± 0.015
Ba-133	0.204 ± 0.004	0.628 ± 0.024	0.526 ± 0.026
Cs-137	0.474 ± 0.010	0.762 ± 0.035	0.525 ± 0.040
Bi-207	0.390 ± 0.002	0.721 ± 0.011	0.526 ± 0.011
Bi-207	0.857 ± 0.008	0.940 ± 0.022	0.511 ± 0.026
Tl-208	2.379 ± 0.004	1.704 ± 0.010	0.514 ± 0.012

Table 5.2 *Results of each sources Compton Edge, Non-relativistic rest energy and Relativistic rest energy.*

5.3 Relativistic Relations

As outlined in section section 2.2.2, multiple values can be further determined from the experimental data. With the use of equations in section 2.2.2, the results of these values for each source can be found in table 5.3.

Source	Electron Velocity (β)	Relativistic Factor (γ)	Total Energy (E)	Momentum (pc)
Na-22	0.796 ± 0.013	1.651 ± 0.047	0.857 ± 0.023	0.682 ± 0.007
Na-22	0.946 ± 0.005	3.076 ± 0.138	1.573 ± 0.020	1.488 ± 0.012
K-40	0.957 ± 0.003	3.432 ± 0.109	1.750 ± 0.013	1.674 ± 0.008
Mn-54	0.895 ± 0.004	2.243 ± 0.044	1.150 ± 0.012	1.029 ± 0.005
Co-56	0.943 ± 0.003	3.014 ± 0.071	1.534 ± 0.011	1.447 ± 0.006
Co-57	0.364 ± 0.032	1.074 ± 0.014	0.569 ± 0.061	0.207 ± 0.006
Co-60	0.938 ± 0.003	2.882 ± 0.068	1.475 ± 0.011	1.383 ± 0.006
Co-60	0.950 ± 0.002	3.192 ± 0.061	1.628 ± 0.009	1.546 ± 0.005
In-116	0.760 ± 0.017	1.539 ± 0.047	0.751 ± 0.026	0.571 ± 0.006
In-116	0.931 ± 0.007	2.734 ± 0.124	1.403 ± 0.021	1.306 ± 0.006
In-116	0.945 ± 0.003	3.063 ± 0.071	1.598 ± 0.011	1.510 ± 0.007
Ba-133	0.694 ± 0.014	1.388 ± 0.027	0.730 ± 0.023	0.506 ± 0.011
Cs-137	0.851 ± 0.015	1.903 ± 0.087	0.999 ± 0.030	0.850 ± 0.006
Bi-207	0.819 ± 0.004	1.741 ± 0.019	0.916 ± 0.010	0.750 ± 0.006
Bi-207	0.928 ± 0.006	2.677 ± 0.101	1.368 ± 0.019	1.269 ± 0.011
Tl-208	0.984 ± 0.001	5.628 ± 0.115	2.893 ± 0.009	2.847 ± 0.004

Table 5.3 *Results each source produced for each of the relativistic relations.*

If the electron velocity, β is plotted on the x-axis against the other relativistic factors an asymptotic relationship should be observed as the electron's velocity tends towards the speed of light the other relativistic will increase as a function of β. While this can be seen from table B.2, the relation is much more evident when plotted.

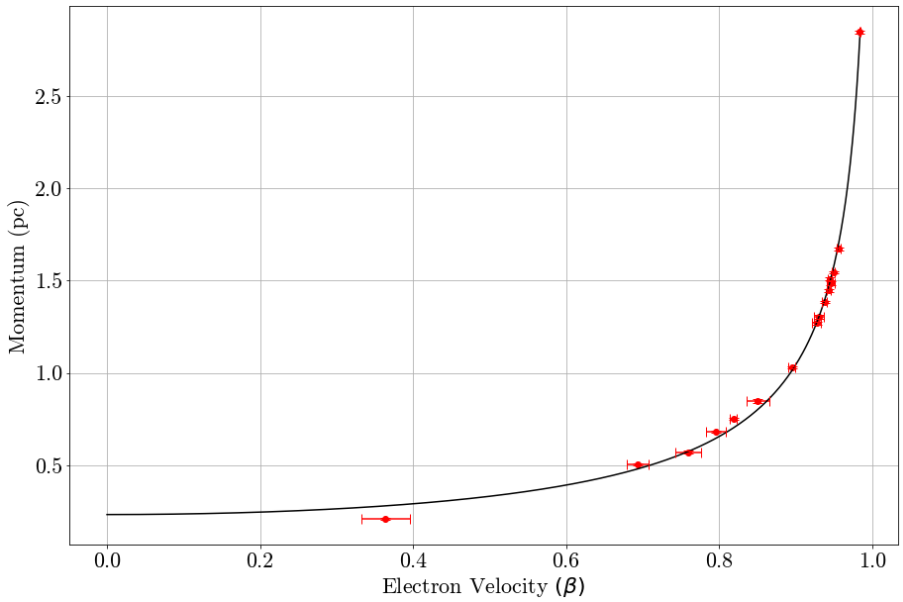

Figure 5.5 *Momentum in MeV plotted against electron velocity.*

As expected fig. 5.5 shows an increase in momentum as the electron velocity increases. While not fully necessary the data was fitted using the expected function as outlined in the lab manual, [7]

$$pc = \gamma\beta m_0 c^2 \tag{5.3}$$

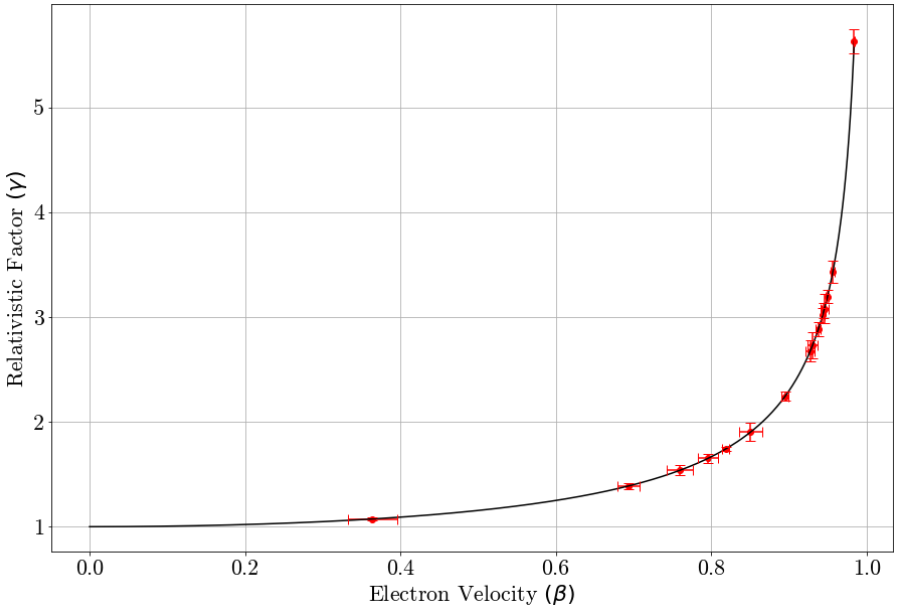

Figure 5.6 *Relativistic factor plotted against electron velocity.*

Similarly in fig. 5.6 the relativistic factor increases as the electron velocity increases, with the expected function fitted as follows,

$$\gamma = \frac{1}{(1-\beta)^{1/2}} \tag{5.4}$$

Finally fig. 5.7 shows the total energy as the electron velocity increases. Once again as expected the total energy increases as expected with the function fitted as follows,

$$E = \frac{m_0 c^2}{\sqrt{1-\beta^2}} \tag{5.5}$$

As expected fig. 5.5, fig. 5.6 and fig. 5.7 all three plots showed a velocity dependence of pc, γ and E when plotted using the Compton edge and independent gamma-ray energy. Each plot also exhibited the asymptotic curve expected as the speed of light is approached as the electron velocity can never succeed the speed of light ($\beta < c$).

The errors plotted here were calculated by propagating the error taken on measurement through relevant equations to each result, this process was completed with the use of an uncertainties package with all relevant code found in appendix D.2. The functions were fitted using SciPy's curve fit function and uncertainties taken on the slopes as the square root of expected diagonals of the covariance matrix.

The size of the errors throughout this section appears to be small compared to the data points. However, due to the nature of the experiment and how the uncertainty was calculated, this is expected.

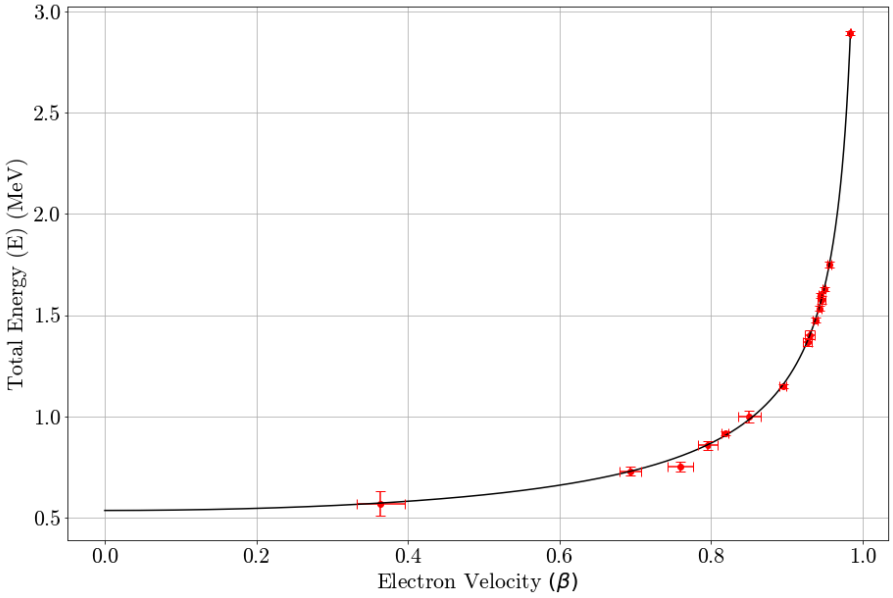

Figure 5.7 *Total energy plotted against electron velocity.*

6 Conclusion

This experiment was dealt with in two-part. The first looked at the gamma rays as they scattered as a function of angle treating them as particles. A linear relationship was found when the inverse of gamma-ray energy (E_γ) was plotted against the scattering angle (θ). The slope and intercept of this linear relationship was found to be $(1.946 \pm 0.007) \times 10^{-26}$ and $(1.573 \pm 0.063) \times 10^{-26}$. This matched the theoretical values of 1.956×10^{-26} and 1.51×10^{-26} very strongly.
The differential cross-section was then calculated for each respective angle and plotted. This showed that the smaller the angle, the higher chance that scattering would occur which is in-line with the theoretical model. This was also compared with the Klein–Nishina method and found in close compliance with the formula's values. However, it was found that that there was an overestimation in the initial experimental data; thus, a correction factor was applied to account for this. [5]

The second part of the investigation investigated the rest energy of the electron for many sources for both non-relativistic and relativistic cases. It was found that when rest energy was determined in the non-relativistic case that a linear relationship was produced with rest energy and the Compton edge. This result was deemed incorrect as the rest energy should fall around the experimentally accepted value for an electrons rest energy of 0.511 MeV. [9] However the y-intercept was found to be 0.518 ± 0.004 MeV. When considering the relativistic case, the rest's mass-energy of the electron was 0.518 ± 0.004 MeV. These results prove that there are shortcomings in the non-relativistic case due to the linear relationship between the Compton edge and rest mass-energy. The uncertainties associated with the values for relativistic rest mass energy were higher than expected, as discussed. When the average rest energy has calculated the uncertainty associated with each value was also propagated, which returned acceptable results.

Finally, relativistic relations as a function of electron velocity were examined. The momentum, relativistic factor, and total energy of the electrons were dependent on the electron velocity with each plot producing asymptotic curves that are in line with the theoretical expectation given by relativity.

References

[1] Arthur H. Compton. "A Quantum Theory of the Scattering of X-rays by Light Elements". In: *Phys. Rev.* 21 (5 May 1923), pp. 483–502. DOI: 10.1103/PhysRev.21.483. URL: https://link.aps.org/doi/10.1103/PhysRev.21.483.

[2] Glenn Frederick Knoll. *Radiation Detection and Measurement*. Wiley, 2000. ISBN: 9780471073383.

[3] Charles M Washington and Dennis T Leaver. *Principles and practice of radiation therapy*. Elsevier, 2016. ISBN: 9780323287524.

[4] Robert J Naumann. *Introduction to the Physics and Chemistry of Materials*. Crc Press, 2009. ISBN: 9781420061338.

[5] *Compton scattering experiment, Advanced Laboratory handout*. Dublin, Ireland: UCD Physics Departmant, 2005.

[6] Kenneth S Krane. *Introductory nuclear physics*. New York, NY: Wiley, 1988. URL: https://cds.cern.ch/record/359790.

[7] P. L. Jolivette and N. Rouze. "Compton scattering, the electron mass, and relativity: A laboratory experiment". In: *American Journal of Physics* 62.3 (1994), pp. 266–271. DOI: 10.1119/1.17611. eprint: https://doi.org/10.1119/1.17611. URL: https://doi.org/10.1119/1.17611.

[8] *AN34 Experiments in Nuclear Science Laboratory Manual fourth edition experiment iv-3 gamma-ray spectroscopy using NaI(Tl)*. Ortec. URL: https://www.ortec-online.com/service-and-support/library/educational-experiments.

[9] S Prasannakumar, S Krishnaveni, and T K Umesh. "Determination of rest mass energy of the electron by a Compton scattering experiment". In: *European Journal of Physics* 33.1 (Nov. 2011), pp. 65–72. DOI: 10.1088/0143-0807/33/1/005. URL: https://doi.org/10.1088/0143-0807/33/1/005.

Appendices

A Constants used throughout investigation

The constants used in eq. (2.6) are as follows,

The following values were determined for the case of ^{137}Cs

$$\alpha = \frac{E_\gamma}{m_0 c^2} = \frac{0.662\text{MeV}}{0.511\text{MeV}} = 1.29$$

In the case of section 5.1 the constants are as follows,

$$\sum_\gamma = \frac{\text{Sum Under Photopeak}}{\text{Counting Time}} \div \text{intrinsic peak efficiency}$$

Where N is the number of electrons in the scattering sample,

$$\begin{aligned} N &= \frac{(\text{mass of scattering rod})(\text{atomic. no})(\text{Avogadro's Number})}{\text{Atomic Mass}} \\ &= \frac{(79.3)(6.022 \times 10^{23})(13)}{27} = 2.299 \times 10^{25} \end{aligned}$$

We also have $\Delta\Omega$ which is the solid angle in the detector in radians.

$$\begin{aligned} \Delta\Omega &= \frac{\text{area of detector } cm^2}{(R_2\ (cm))} \\ &= \frac{\pi 26^2}{2} = 4.650 \times 10^{-3} \end{aligned}$$

Where the I, incident gamma rays per unit area is given by,

$$\begin{aligned} I &= 1.013 \times 10^6 \exp(-t/43.48)\ \text{Bq cm}^{-2} \\ &= 1.013 \times 10^6 \exp(-42.58/43.48) \\ &= 380429.805\ \text{Bq cm}^{-2} \end{aligned}$$

Constant	Value
α	1.29
Electron Radius (r_0)	2.820×10^{-13} cm
Detector Radius (r_d)	1 cm
Incident Gamma Rays (I)	380429.805 Bq cm^{-2}
Time in years from August 1977 to March 2020	42.583 years
Solid detector angle ($\Delta\Omega$)	4.650×10^{-3}
Scattering rod mass (M_s)	79.3 g
Sample to detector distance (R_2)	26 cm
Number of electrons within the scattering sample	2.299×10^{25}

B Raw Data

As stated at the start of the report, all data was provided by the University College Dublin school of Physics. The data was taken in March of 2020.

Angle (θ)	Counting Time (s)	Scattered Gamma Ray Energy (E_γ)(keV)	Photopeak Net Area
20	158.56	597 ± 56	12616 ± 343
25	221.78	573 ± 65	15240 ± 430
30	290.38	549 ± 55	17925 ± 456
35	208.42	518 ± 50	10484 ± 368
40	318.50	487 ± 54	15680 ± 467
45	307.54	470 ± 55	13043 ± 437
50	390.84	439 ± 54	14791 ± 499
55	706.66	416 ± 52	24188 ± 598
60	446.52	390 ± 49	14105 ± 474
65	466.00	371 ± 44	14757 ± 460
70	359.30	348 ± 41	10067 ± 393
75	713.38	332 ± 38	19027 ± 470
80	467.74	316 ± 37	11828 ± 383
85	420.62	300 ± 35	10227 ± 347
90	3029.70	284 ± 35	73551 ± 1082

Table B.1 *Data obtained from carrying out experiment in the lab for the first part of the experiment.*

Sources	Photopeak (E_γ)(keV)	Compton Edge (T)(keV)
Na-22	510 ± 2	338 ± 6
Na-22	1275 ± 2	1062 ± 10
K-40	1457 ± 2	1240 ± 7
Mn-54	833 ± 2	637 ± 4
Co-56	1236 ± 2	1025 ± 5
Co-57	123 ± 2	39 ± 3
Co-60	1173 ± 2	963 ± 5
Co-60	1332 ± 2	1118 ± 4
In-116	417 ± 2	263 ± 6
In-116	1098 ± 2	890 ± 10
In-116	1293 ± 2	1076 ± 5
Cs-137	662 ± 2	474 ± 10
Bi-207	570 ± 2	390 ± 2
Bi-207	1063 ± 3	857 ± 8
Tl-208	2613 ± 3	2379 ± 4

Table B.2 *Data obtained from carrying out experiment in the lab for the second part of the experiment.*

C Derivation of Compton Scattering Equation

Keeping in mind the situation depicted in fig. 2.1 and using the Planck relationship and the relativistic energy expression, conservation of energy takes the form,

$$h\nu_i + m_e c^2 = h\nu_f + \sqrt{p_e^2 c^2 + m_e^2 c^4} \tag{C.1}$$

Conservation of momentum requires,

$$\vec{p_i} = \vec{p_f} + \vec{p_e} \tag{C.2}$$

Where $p = E/c$ is used for the photon momentum. Squaring this equation using the scalar product gives,

$$p2_e = (p_i - p_f) \cdot (p_i - p_f) = p_i^2 + p_f^2 - 2p_i p_f \cos\theta \tag{C.3}$$

Again using the Planck relationship and the relativistic energy expression, multiplied by c^2 and substituting $pc = h\nu$,

$$(p_e c)^2 = (h\nu_i)^2 + (h\nu_f)^2 - 2h^2 \nu_i \nu_f \cos\theta \tag{C.4}$$

The energy conservation expression above can be squared to give,

$$(p_e c)^2 = (h\nu_i)^2 + (h\nu_f)^2 - 2h^2 \nu_i \nu_f + 2m_e c^2 (h\nu_i - h\nu_f) \tag{C.5}$$

Rearranging,

$$\frac{1}{h\nu_f} - \frac{1}{h\nu_i} = \frac{1}{m_e c^2}(1 - \cos\theta) \tag{C.6}$$

finally the standard form of the Compton formula is obtained,

$$\lambda_f - \lambda_i \; = \; \Delta\lambda \; = \frac{h}{m_e c}(1 - \cos\theta) \tag{C.7}$$

Note: This derivation is directly paraphrased from HyperPhysics and can be found at the following link, `http://hyperphysics.phy-astr.gsu.edu/hbase/quantum/compeq.html`

D Relevant Code Used

```
import numpy as np
import pandas as pd
import math
import uncertainties
from uncertainties import ufloat_fromstr
from uncertainties import unumpy as unp
import matplotlib.mlab as mlab
import matplotlib.pyplot as plt
from scipy import stats
from scipy . optimize import curve_fit
from scipy . interpolate import interp1d
from scipy import optimize

# ---- plot parameters ----
plt.rcParams["figure.figsize"] = (15,10)
plt.rc('font', family = 'serif', serif = 'cmr10')
plt.rcParams.update({'font.size': 22})
```

Listing 1 *Package Import*

```
    # ---- Importing data from .csv ----

    # ---- Importing data from table 1 provided in raw data word document ----

    part_1 = pd.read_csv('data\Compton_scattering_formula_and_differential_cross_section.csv')

    part_2 = pd.read_csv('data\compton_scattering_electron_mass_rel.csv')
```

Listing 2 *Importing data*

D.1 Code used for evaluation of scattered gamma ray energies and cross section.

```
    # ---- Variable Definition ----

    # ---- Part 1 ----

    angle = part_1['Angle']
    counts_time = np.array(part_1['Counting_time'])
    gamma_ray_energy = part_1['scattered_gamma_ray_energy']
    gamma_ray_uncer = part_1['scattered_gamma_ray_energy_uncer']
    photopeak_area = part_1['photopeak_net_area']
    photopeak_uncer = part_1['photopeak_net_area_uncer']

    # ---- conversion and uncertainty coupling ----



    angle = unp.uarray(angle, 1)
    gamma_rays = unp.uarray(gamma_ray_energy, gamma_ray_uncer) 0.001 # conversion from KeV to MeV
```

```
photopeak = unp.uarray(photopeak_area, photopeak_uncer)

print(photopeak)

angle_r = angle (np.pi/180)
```

Listing 3 *Variable Defnition for data analysis*

```
# -- function definition --

def lin_func(x, m, c):
    return m x + c #equation of a line y = mx + c

def exp(x, a, b):
    return a np.exp(-b x)

# - differential cross section -

def Klein_Nishina(theta):
    r = 2.82e-13
    alpha = 1.29
    A = (r 2/2) ((1 + np.cos(theta) 2)/(1 + alpha (1 - np.cos(theta) 2)))
    t = (alpha 2) (1 - np.cos(theta)) 2
    b = (1 + np.cos(theta) 2) (1 + alpha (1 - np.cos(theta)))
    B = t/b
    return A B


def gamma_sum(energy, photopeak, counting_time):
    peak_eff = .1522(energy) -1.1325
    return (photopeak/counting_time)/peak_eff


def diff_cross(gamma_sum):
    t = 42.583 # time in years from August of 1977 to March 2020, when data was taken.
    I = 1.013e6 np.exp(-t/43.48)
    delta_omega = np.pi/26 2
    N = ((79.3)(6.0221409e+23)(13))/27
    return gamma_sum/(I delta_omega N)

def KleinNishina (ang) : #in cm squared / steradians
    alpha = 1.29
    r = 2.82e-13
    return ((r 2) /2)((1+(np.cos(ang)) 2)/(1+((alpha)(1 - np.cos(ang)))) 2)(1+( (alpha
        2) ((1 - np.cos(ang)) 2) /( (np.cos(ang)) 2)(1+((alpha)(1 - np.cos(ang))))))
```

Listing 4 *Function defintion*

```
# -- Slope of Curve --

print('The slope of the above curve is:', "{:.3f}".format(popt1[0]))

# -- Finding Intercept --
```

```
x = 0
y = (popt1[0] x) + popt1[1]
print('y-intercept of the line:', "{:.3f}".format(y))

# ---- Comparison with theoretical values ----

print('The slope of the fitted data is', "{:.3f}".format(1.956/popt1[0] - 1),'% greater than
    predicted value for slope.')

xth = 0
yth = (1.956 x) + 1.51
print('y-intercept of the theoretical line is:', "{:.3f}".format(yth))

print('y-intercept of the fitted data is', "{:.3}".format(y/yth - 1),'% greater than predicted
    value for slope.')


# ---- Uncetainties on the Slope ----


print('Uncertainty on the y-intercept is given as,', "{:.3}".format(np.sqrt(pcov1[0][0])))
print('Uncertainty on the slope is given as,', "{:.3}".format(np.sqrt(pcov1[1][1])))


# ---- Final Values are Given by ----

print("Intercept: ", "{:.3f}".format(y), '+-', "{:.2}".format(np.sqrt(pcov1[0][0])))
print("Slope: ", "{:.3f}".format(popt1[0]), '+-', "{:.1}".format(np.sqrt(pcov1[1][1])))
```

```
# ---- data for graph ----

x = unp.nominal_values(angle_r)
xerr = unp.std_devs(angle_r)

p1 = gamma_sum(gamma_rays, photopeak, counts_time)
# print(p1)
p2 = diff_cross(p1)
# print(p2)


# ---- theortical model ----

yth = KleinNishina(x)

# --
correction_factor = (yth/p2).mean()
# --

p2 = diff_cross(p1) correction_factor

y = unp.nominal_values(p2)
y_err = unp.std_devs(p2)
```

```
# ---- fitting function ----

x_s = np.linspace(x.min() - .1, x.max(), 1000)

popt1, pcov1 = curve_fit(exp, x, y, sigma = y_err, absolute_sigma = True, p0 = [1e-26, 2])
fit_data = exp(x_s, popt1[0], popt1[1])

# ----

popt2, pcov2 = curve_fit(exp, x, yth, p0 = [7e-26, .7])
th_data = exp(x_s, popt2[0], popt2[1])

# ---- Plotting ----

plt.plot(x_s, th_data, label = 'Theortical Prediction', color = 'blue')
plt.scatter(x, y, label = 'Data Points ', color = 'red')
plt.plot(x_s, fit_data, label = 'Corrected Data Fit', color = 'black')
plt.errorbar(x, y, xerr = xerr, yerr = y_err, capsize= 5, ls='none', color = 'red')

plt.xlabel('Angle $(\phi )$, (Radians)')
plt.ylabel('Differential Cross Section')

plt.legend()
plt.grid()
plt.savefig('images/angle_vs_cross_section.png')
```

```
# ---- Variable Compile ----

x = unp.nominal_values(angle_r)
xerr = unp.std_devs(angle_r)
yth = KleinNishina(x)
y = unp.nominal_values(p2)
y_err = unp.std_devs(p2)
percent = (y/yth - 1) 100
# print(percent)

print(stats.chisquare(f_obs=y, f_exp=yth))

# ---- write to .csv ----

Output = [x, xerr, y 1e26, y_err 1e26, yth 1e26, percent]

# print(Output)
dataset = pd.DataFrame({'Angle': np.round(Output[0], 3), 'Angle_Error': np.round(Output[1], 3)
    , 'Diff_Cross_Section': np.round(Output[2], 3), 'Diff_Cross_Section_Uncer': np.round(
    Output[3], 3), 'Diff_Cross_Section_Th': np.round(Output[4], 3), 'Percent': np.round(
    Output[5], 1)})
print(dataset)

print(dataset.to_latex(index=False))
dataset.to_csv('data/theor_compare.csv')
```

D.2 Code used for investigating relativistic relations

```
    # ---- Loading Data ----

    sources = part_2['Source']
    photopeak = part_2['Photopeak']
    photopeak_uncer = part_2['Photopeak_Uncertainty']
    compton_edge = part_2['Compton_Edge']
    compton_edge_uncer = part_2['Compton_Edge_Uncertainty']

    # ---- converting data and coupling ----

    photopeak = unp.uarray(photopeak, photopeak_uncer) 0.001
    compton_edge = unp.uarray(compton_edge, compton_edge_uncer) 0.001
```

```
    x = unp.nominal_values(photopeak)
    y = unp.nominal_values(compton_edge)
    x_err = unp.std_devs(photopeak)
    y_err = unp.std_devs(compton_edge)

    # ---- Fitting ----

    popt1, popc1 = curve_fit(lin_func, x, y)
    fit_data = lin_func(x, popt1[0], popt1[1])

    # ---- Plotting ----

    plt.scatter(x, y, color = 'red')
    plt.errorbar(x, y, xerr = x_err, yerr = y_err, capsize= 5, ls='none', color = 'red')
    plt.plot(x, fit_data, color = 'black')
    plt.grid()
    plt.xlabel('Photopeak (MeV)')
    plt.ylabel('Compton Edge (MeV)')
    plt.savefig('images/photo_peak_vs_compton_edge.png')
```

```
    # ---- Slope of Curve ----

    print('The slope of the above curve is:', "{:.3f}".format(popt1[0]))

    # ---- Finding Intercept ----

    x = 0
    y = (popt1[0] x) + popt1[1]
    print('y-intercept of the line:', "{:.3f}".format(y))
```

```
    def classical_energy(gamma_energy, compton_edge):
    return ((2 gamma_energy - compton_edge) 2) /(2 compton_edge)

def rel_energy(gamma_energy, compton_edge):
    return 2 gamma_energy (gamma_energy - compton_edge)/compton_edge
```

```
x = unp.nominal_values(compton_edge)
x_err = unp.std_devs(compton_edge)

clre = classical_energy(photopeak, compton_edge)

y = unp.nominal_values(clre)
y_err = unp.std_devs(clre)

# —— Fitting ——

popt1, popc1 = curve_fit(lin_func, x, y)
fit_data = lin_func(x, popt1[0], popt1[1])

plt.plot(x, fit_data, color = 'black')
plt.scatter(x, y, color = 'red')
plt.errorbar(x, y, xerr = x_err, yerr = y_err, capsize= 5, ls='none', color = 'red')
plt.xlabel('T (MeV)')
plt.ylabel('$mc^2$ (MeV)')
plt.grid()
plt.savefig('images/electron_cl.png')
```

```
# —— Slope of Curve ——

print('The slope of the above curve is:', "{:.3f}".format(popt1[0]))

# —— Finding Intercept ——

x = 0
y = (popt1[0]x) + popt1[1]
print('y-intercept of the line:', "{:.3f}".format(y))
```

```
x = unp.nominal_values(compton_edge)
x_err = unp.std_devs(compton_edge)

relre = rel_energy(photopeak, compton_edge)
ovr_err = relre.mean()

y = unp.nominal_values(relre)
y_err = unp.std_devs(relre)

# —— Accepted Value of rest mass ——
#0.5110 MeV

plt.axhline(y = 0.511, color = 'green', alpha = .7, label = 'Experimentally Accepted Value')

# —— comparing to average values ——

plt.axhline(y = y.mean(), color = 'purple', alpha = .7, label = 'Average Value of Data')

plt.scatter(x, y, color = 'red')
plt.errorbar(x, y, xerr = x_err, yerr = y_err, capsize= 5, ls='none', color = 'red')
plt.grid()
```

```
    plt.xlabel('T (MeV)')
    plt.ylabel('$mc^2$ (MeV)')
    plt.legend()
    plt.savefig('images/electron_rel.png')
```

```
    print('Average rest energy', '{:.3f}'.format(ovr_err), 'MeV')
    print('The difference in rest energy between experimental data and the accepted value is', '
        {:.3f}'.format(y.mean() - 0.511), 'MeV, this is a differnce of', '{:.3f}'.format(0.511/y.
        mean()), '%')
    print('Errors on the y-values',  '{:.3f}'.format(y_err.mean()))
```

```
    def electron_velocity(E, T):
    return (T (2 E - T))/(T 2 - 2 E T + 2 E 2)

def relativistic_factor(E, T):
    return 1 + ((T 2)/(2 E (E - T)))

def total_energy(E, T):
    return (T 2 - 2 T E + 2 E 2)/(T)

def momentum(E, beta):
    return E beta

def unique_fit(x, a, b, c):
    return 1/np.sqrt(a + b x 2) + c
```

```
    beta = electron_velocity(photopeak, compton_edge)
    gamma = relativistic_factor(photopeak, compton_edge)
    E = total_energy(photopeak, compton_edge)
    pc = momentum(E, beta)


    # ---- Writing data to CSV ----

    Output = [sources, unp.nominal_values(beta), unp.std_devs(beta), unp.nominal_values(gamma),
        unp.std_devs(gamma), unp.nominal_values(clre), unp.std_devs(clre), unp.nominal_values(
        relre), unp.std_devs(relre), unp.nominal_values(E), unp.std_devs(E)]

    # print(Output)
    dataset = pd.DataFrame({'Source': Output[0], 'beta_values': np.round(Output[1], 3), '
        beta_uncertainties': np.round(Output[2], 3), 'Gamma_values': np.round(Output[3], 3), '
        Gamma_uncertainties': np.round(Output[4], 3), 'Classical_Rest_Energy_MeV': np.round(
        Output[5], 3), 'Classical_Rest_Energy_uncertainties_MeV': np.round(Output[6], 3), '
        Relativistic_Rest_Energy_MeV': np.round(Output[7], 3), '
        Relativistic_Rest_Energy_uncertainties_MeV': np.round(Output[8] , 3), 'Total_Energy': np.
        round(Output[9], 3), 'Total_Energy_Uncer': np.round(Output[10], 3)})
    # print(dataset)
    print(dataset.to_latex(index=False))
    dataset.to_csv('data/relativistic_relations.csv')
```

```
    x = unp.nominal_values(beta)
    y = unp.nominal_values(pc)
```

```
    x_err = unp.std_devs(beta)
    y_err = unp.std_devs(pc)

    plt.ylabel('Momentum (pc)')
    plt.xlabel('Electron Velocity $( \\beta )$')

    # ---- fitting function ----

    x_s = np.linspace(0, x.max(), 1000)

    popt1, pcov1 = curve_fit(unique_fit, x, y, sigma = y_err, absolute_sigma = True, p0 = [.1, 3,
        1])
    fit_data = unique_fit(x_s, popt1[0], popt1[1], popt1[2])

    plt.plot(x_s, fit_data, color = 'black')
    plt.scatter(x, y, color = 'red')
    plt.errorbar(x, y, xerr = x_err, yerr = y_err, capsize= 5, ls='none', color = 'red')
    plt.grid()
    plt.savefig('images/pc_vs_Velocity')
```

```
    x = unp.nominal_values(beta)
    y = unp.nominal_values(gamma)
    x_err = unp.std_devs(beta)
    y_err = unp.std_devs(gamma)

    # ---- fitting function ----

    x_s = np.linspace(0, x.max(), 1000)

    popt1, pcov1 = curve_fit(unique_fit, x, y, sigma = y_err, absolute_sigma = True, p0 = [.1, 3,
        1])
    fit_data = unique_fit(x_s, popt1[0], popt1[1], popt1[2])

    plt.plot(x_s, fit_data, color = 'black')

    plt.scatter(x, y, color = 'red')
    plt.errorbar(x, y, xerr = x_err, yerr = y_err, capsize= 5, ls='none', color = 'red')

    plt.grid()
    plt.ylabel('Relativistic Factor $(\gamma)$')
    plt.xlabel('Electron Velocity $( \\beta )$')
    plt.savefig('images/RelFactor_vs_Velocity')
```

```
    x = unp.nominal_values(beta)
    y = unp.nominal_values(E)
    x_err = unp.std_devs(beta)
    y_err = unp.std_devs(E)

    # ---- fitting function ----

    x_s = np.linspace(0, x.max(), 1000)
```

```
    popt1, pcov1 = curve_fit(unique_fit, x, y, sigma = y_err, absolute_sigma = True, p0 = [.1, 3,
        1])
    fit_data = unique_fit(x_s, popt1[0], popt1[1], popt1[2])

    plt.plot(x_s, fit_data, color = 'black')

    plt.scatter(x, y, color = 'red')
    plt.errorbar(x, y, xerr = x_err, yerr = y_err, capsize= 5, ls='none', color = 'red')

    plt.grid()
    plt.ylabel('Total␣Energy␣(E)␣(MeV)')
    plt.xlabel('Electron␣Velocity␣$(␣\\beta␣)$')
    plt.savefig('images/TE_vs_Velocity')
```